Multi-contrast computed laminography at ANKA light source

Y Cheng[1,2], V Altapova[3], L Helfen[1,4], F Xu[1], T dos Santos Rolo[1], P Vagovič[1], M Fiederle[2] and T Baumbach[1,3]

[1] Institute for Photon Science and Synchrotron Radiation /ANKA light Source, Karlsruhe Institute of Technology (KIT), D-76344 Karlsruhe, Germany
[2] Freiburger Materialforschungszentrum (FMF), University of Freiburg, D-79104 Freiburg, Germany
[3] Laboratory for Applications of Synchrotron Radiation (LAS), Karlsruhe Institute of Technology (KIT), Postfach 6980, D-76128 Karlsruhe, Germany
[4] European Synchrotron Radiation Facility (ESRF), F-38043 Grenoble, France

E-mail: yin.cheng@kit.edu

Abstract. X-ray computed laminography has been developed as a non-destructive imaging technique for inspecting laterally extended objects. Benefiting from a parallel-beam geometry, high photon flux of synchrotron sources and modern high-resolution detector systems, synchrotron radiation computed laminography (SRCL) results in a powerful three-dimensional microscopy technique. SRCL can be combined with different contrast modes, such as absorption, phase and dark-field contrasts, in order to provide complementary information for the same specimen. Here we show the development of SRCL at the TopoTomo beamline of the ANKA light source. A novel instrumentation design is reported and compared to the existing one. For this design, experimental results from different contrast modalities are shown.

1. Introduction

Computed laminography using synchrotron radiation has been developed as a non-destructive three-dimensional (3-D) imaging method for planar specimens [1]. Compared with its laboratory counterparts, a parallel-beam geometry and high flux enables fast and monochromatic imaging with high resolution. In comparison to computed tomography (CT), SRCL is based on the inclination of the tomographic rotation axis with respect to the incident X-ray beam by a defined angle, the so-called laminographic angle θ. In other words, $\theta = 90°$ and $\theta = 0°$ are the limiting cases of CT and radiography, respectively.

SRCL provides a possibility to zoom into regions of interest (ROIs) of macroscopically large specimens with microscopic resolution without affecting their integrity. Originally it has been motivated by and developed for non-destructive microsystem device inspection [2, 3]. Recently, the technique has been extended to applications in materials science [4, 5], paleontology [6] and cultural heritage [7]. Nowadays by exploiting the high degree of coherence of the synchrotron beam, applications of SRCL have been further broadened by their combination with phase-contrast imaging methods and microscopy techniques [8, 9, 10].

In this paper, we will report on the development of SRCL at ANKA's TopoTomo beamline.

2. Principles and Instrumentation Design

The TopoTomo beamline at ANKA is a micro-imaging station dedicated to topography and tomography with a maximum beam cross section of 5 mm × 15 mm (V×H, FWHM) at the sample position 30 m downstream of the bending magnet source [11]. For typical imaging applications, a filtered white beam or a double-multilayer monochromator provides x-ray energies of 5 ∼ 30 keV. The combination of different scintillator crystals and microscope optics yields a large flexibility in spatial resolution values (pixel sizes from 0.36 to 6.1 μm).

A schematic drawing in Figure 1(a) depicts the basic principle of SRCL. In order to realize the SRCL geometry, an accurate inclination of the sample rotary stage with respect to the X-ray beam has to be performed. To guarantee a large freedom of the laminographic angle θ, two designs have been proposed (see Figure 1(b),(c)). The Design I (Figure 1(b)) is a novel design which utilizes a horizontal rotation by using an additional rotary stage to enable a full circular tilting (theoretically) of the sample stage. The Design II (Figure 1(c)) realizes the tilting of the sample stage by simply using a goniometer stage together with a fixing angle wedge (details of Design II has been demonstrated elsewhere [12]). Both designs have advantages and drawbacks. Comparing the degrees of freedom (DOF) for both designs, the novel Design I has a flexible inclination angle range from -180° to +180°, which allows one to perform radiography ($\theta = 0°$) if there is an aperture through the sample rotary stage. The Design II only allows an accessible inclination angle range of 0° to +32° (limited by the travel range of the goniometer).

Since both designs can complement each other and fit to different requirements or conditions, both have been implemented at the TopoTomo beamline. Figure 1(d), (e) show experimental implementations that correspond to Design I (b) and Design II (c), respectively.

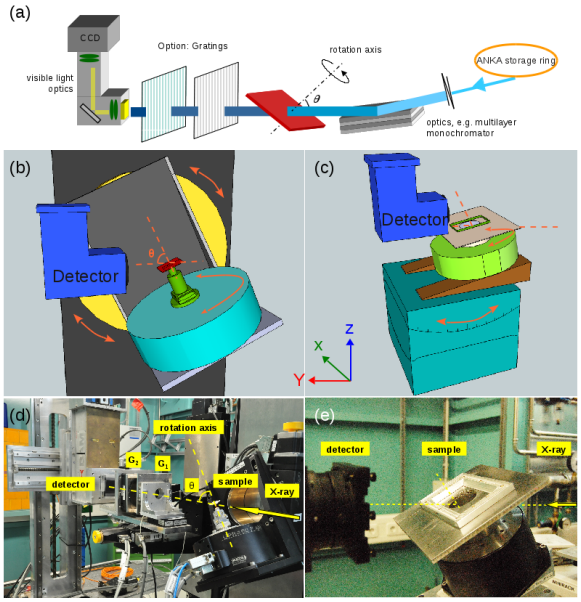

Figure 1. (a) Principle of CL at synchrotron beamlines with parallel-beam geometry. (b)(c) 3-D drawings of the different proposed designs for the SRCL sample manipulator. (d)(e) Experimental setup corresponding to Designs I (b) and II (c) respectively. Both are implemented at the TopoTomo beamline.

3. Multi-contrast SRCL

Similar to CT, SRCL can be combined with diverse contrast modes, including inline phase-contrast and Talbot interferometry in addition to the traditional absorption contrast. In the following, various contrast modalities for SRCL at the TopoTomo beamline will be illustrated by an example.

3.1. Absorption and inline phase-contrast modalities

A wavefront of spatially coherent hard X-rays becomes distorted when it penetrates an object. It undergoes not only attenuation (related to the imaginary part β of the complex refractive index) but also a phase shift, caused by the non-uniform distribution of the refractive index decrement δ in the sample. While the attenuation results in an intensity modulation behind the object, the phase distortion develops into intensity modulations only as the wave continues to propagate (provided that there is sufficient partial coherence). In the hard X-ray region, δ is orders of magnitude higher than β for light materials. Therefore, by changing the sample to detector distance we can achieve absorption laminography for attenuating materials or inline phase-contrast laminography for weakly absorbing materials.

To demonstrate the resolution achievable via SRCL at TopoTomo, we imaged a test pattern (Xradia Inc., Concord, CA) in absorption mode (Figure 2). An axis inclination angle of around 30° ($\theta \approx 60°$) and a monochromatic beam of 17 keV X-ray energy were used. Volumes were reconstructed from 1599 projections (4 s exposure time) using filtered backprojection [12].

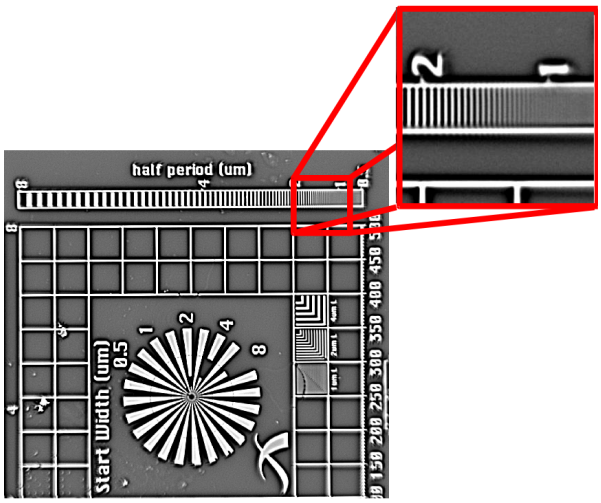

Figure 2. Reconstructed slice of Xradia resolution test pattern (X500-200-2). A zoom-in region shows that the in-plane spatial resolution allows one to distinguish features smaller than 1.5 μm size. The effective pixel size was 0.36 μm.

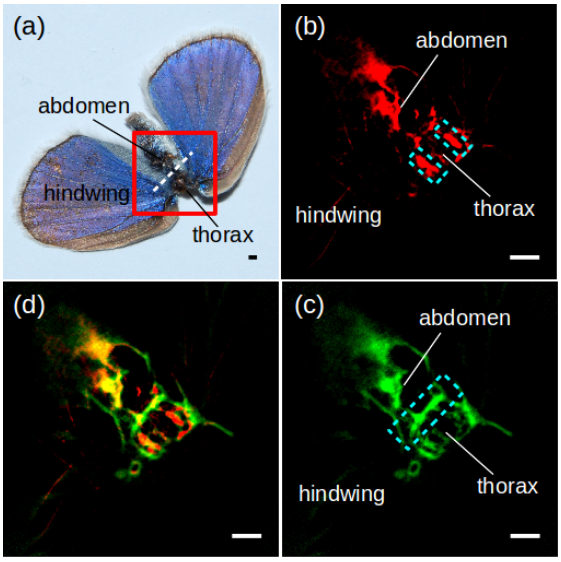

Figure 3. Images of a butterfly (*Pararge aegeria*). (a) the photograph. (b) slice of reconstructed transmission image. (c) slice of the dark-field image. (d) a signal map combining absorption (red) and dark-field (green). The effective pixel size is 6.1 μm. Scale bars: 1 mm.

3.2. Grating interferometry based modality

The grating interferometry (GI) technique is based on the Talbot effect and consists of a phase grating (G_1) and an amplitude grating (G_2), for details of this method see Refs [13, 14]. It has received great attention as a highly sensitive phase-contrast technique, providing simultaneously absorption, phase and dark-field contrast modes. Subsequently, GI-based CT has been conducted mostly for biological applications [15]. The principle of GI-based SRCL [16, 17] has already been shown in Figure 1(d). The pair of gratings is positioned downstream of the sample. We use the phase-stepping method to retrieve the absorption, differential phase and dark-field signals of the sample.

Figure 3 shows slices through the reconstructed volume of a butterfly (red box in Figure 3(a)) scanned by GI-based SRCL. The X-ray energy was chosen to 18 keV monochromatic beam, the laminographic angle was $\theta \approx 60°$. As before, 1599 projections have been taken with 4 s exposure time per projection. Phase-stepping has been conducted by moving the phase grating G_1 over 1 period using 4 steps.

From the comparison of the absorption image (Figure 3(b)) and dark-field image (Figure 3(c)) (the differential phase-contrast image not shown here), we see that at the interface of the thorax and abdomen (cyan box in Figure 3(c)), where only thin nerves, ducts or vessels are passing, shows a very strong scattering signal rather than absorption. While at the wing bases where the two wings attach to the thorax on each side (cyan box in Figure 3(b)), it shows strong absorption due to relatively heavy chitinous compositions rather than showing scattering contrast. These complementary information are visualised in a combined signal map showing in Figure 3(d).

4. Conclusion

SRCL has been successfully implemented at the TopoTomo beamline of the ANKA light source, KIT, Germany. Equipped with a double multilayer monochromator, a pink beam with a spectral bandwidth of $\triangle$E/E=10^{-2} can be obtained to perform μm-scale inline phase-contrast laminography with energies up to 30 keV. By combining CL with grating interferometry, high-sensitivity dark-field contrast of flat specimens can be achieved. These flexible combinations allow a complementary investigation of laterally extended objects. Multi-contrast SRCL is under operation and opens up new possibilities for 3D imaging in life and material sciences.

Acknowledgments

Many thanks go to Harald Schade, Stefan Uhlemann, Thorsten Müller, Jan Psariotis and Gernot Buth for beamline support. Arndt Last and the use of KNMF Facility are acknowledged for precisely fixing the resolution pattern onto its holder. Yin Cheng would like to thank Yang Yang and acknowledges financial support by the CSC-Helmholtz Scholarship Program.

References

[1] Helfen L, Baumbach T, Mikulík P *et al.* 2005 *Appl. Phys. Lett.* **86** 071915
[2] Helfen L, Myagotin A, Pernot P, DiMichiel M, Mikulík P, Berthold A and Baumbach T 2006 *Nucl. Inst. Meth. A* **563** 163–166
[3] Tian T, Xu F, Han J K, Choi D, Cheng Y, Helfen L, Di Michiel M, Baumbach T and Tu K N 2011 *Appl. Phys. Lett.* **99** 082114
[4] Moffat A J, Wright P, Helfen L *et al.* 2010 *Scr. Mater.* **62** 97
[5] Morgeneyer T, Helfen L, Sinclair I, Proudhon H, Xu F and Baumbach T 2011 *Scripta Mater.* **65** 1010 – 1013
[6] Houssaye A, Xu F, Helfen L, De Buffrnil V, Baumbach T and Tafforeau P 2011 *J. Vertebr. Paleontol.* **31** 2–7
[7] Krug K, Porra L, Coan P, Wallert A, Dik J, Coerdt A, Bravin A, Elyyan M, Reischig P, Helfen L and Baumbach T 2008 *J. Synchrotron Rad.* **15** 55–61
[8] Helfen L, Baumbach T, Cloetens P and Baruchel J 2009 *Appl. Phys. Lett.* **94** 104103
[9] Xu F, Helfen L, Moffat A J, Johnson G, Sinclair I and Baumbach T 2010 *J. Synchrotron Rad.* **17** 222–226
[10] Xu F, Helfen L, Suhonen H, Elgrabli D, Bayat S, Reischig P, Baumbach T and Cloetens P 2012 *PLoS ONE* **7** e50124
[11] Rack A *et al.* 2009 *Nucl. Instrum. Meth. B* **267** 1978 – 1988
[12] Helfen L, Myagotin A, Mikulík P, Pernot P, Voropaev A, Elyyan M, Di Michiel M, Baruchel J and Baumbach T 2011 *Rev. Sci. Instrum.* **82** 063702
[13] Momose A, Kawamoto S, Koyama I, Hamaishi Y, Takai K and Suzuki Y 2003 *Jpn. J. Appl. Phys.* **42** L866–L868
[14] Weitkamp T, Diaz A, David C, Pfeiffer F, Stampanoni M, Cloetens P and Ziegler E *Opt. Express* 6296–6304
[15] Momose A, Yashiro W, Takeda Y, Suzuki Y and Hattori T 2006 *Jpn. J. Appl. Phys.* **45** 5254–5262
[16] Harasse S, Hirayama N, Yashiro W and Momose A 2010 *Proc. SPIE* **7804** 780411
[17] Altapova V, Helfen L, Myagotin A, Hänschke D, Moosmann J, Gunneweg J and Baumbach T 2012 *Opt. Express* **20** 6496–6508